Author Manuscript

Authors: Daniel Aaron Holland-Moritz; Michael Wismer; Benjamin Mann; Iman Farasat; Erik Guetschow; Shuwen Sun; Jeffrey Moore; Robert Kennedy; Ian Mangion; Christopher J Welch; Paul Devine

Mass Activated Droplet Sorting (MADS) Enables High Throughput Screening of Enzymatic Reactions at Nanoliter Scale

Daniel A. Holland-Moritz,[a] Michael Wismer,[b] Benjamin F. Mann,[c] Iman Farasat,[d] Paul Devine,[c] Erik D. Guetschow,[c] Ian Mangion,[c] Christopher J. Welch,[e] Jeffrey C. Moore,*[c] Shuwen Sun,*[c] and Robert T. Kennedy*[a]

Abstract: Microfluidic droplet sorting enables the high throughput screening and selection of water-in-oil microreactors at speeds and volumes unparalleled by traditional well-plate approaches. Most such systems sort using fluorescent reporters on modified substrates or reactions that are rarely industrially relevant. We describe a microfluidic system for high throughput sorting of nanoliter droplets based on direct detection using electrospray ionization mass spectrometry (ESI-MS). Droplets are split, one portion is analyzed by ESI-MS, and the second portion is sorted based on the MS result. Throughput of 0.7 samples/s is achieved with 98% accuracy using a self-correcting and adaptive sorting algorithm. We use the system to screen ~15,000 samples in 6 h and demonstrate its utility by sorting 25 nL droplets containing transaminase expressed *in vitro*. Label-free ESI-MS droplet screening expands the toolbox for droplet detection and recovery, improving the applicability of droplet sorting to protein engineering, drug discovery, and diagnostic workflows.

Introduction

Droplet microfluidics enables experiments to be performed at nanoliter to femtoliter scale, increasing throughput and decreasing unit costs of chemical and biological experimentation.[1, 2] A decade of research in the field has demonstrated the utility of droplet systems for a range of applications, including single cell gene expression profiling,[3] small molecule screening,[4] and diagnostics.[5] Dielectrophoretic (DEP) droplet sorting[6] has made possible the rapid recovery of selected samples for analysis.[7, 8] The ability of microfluidic systems to create, assay, and sort microscale samples is attractive in applications where sample preparation and analysis are bottlenecks, e.g. directed evolution of enzymes.

Active sorting of microfluidic droplets largely relies on optical detection.[9, 10] Fluorescence activated droplet sorting (FADS) is most frequently utilized because of its high speed and sensitivity. FADS has found use in ultrahigh throughput screening for directed evolution.[11-13] Screening large libraries is often the rate-limiting step in biocatalyst development, where thousands of enzyme variants must be tested for catalytic activity,[2] and plate based screens are time and resource intensive. FADS has enabled screening of libraries containing millions of variants in a few hours.

Fluorescence detection requires a reporter molecule, a condition that is difficult to meet in many applications.[14, 15] Fluorescent indicators must be carefully selected to ensure that they are retained within droplets,[16, 17] do not interfere with the process being investigated, and provide a readout dependent only upon the assay of interest. These limitations have restricted the use of droplet assays for high throughput biocatalyst screening in industry, where most target analytes are small molecule pharmaceuticals that are difficult to adapt to fluorescent assays. For example, in developing a transaminase for the production of the pharmaceutical sitagliptin, Savile et. al[18] screened nearly 36,000 variants of a transaminase. HPLC-MS was used to guide the selection of variants because the transformation (ketone to chiral amine) produced no significant change in the optical properties of the substrate and product.

To address the limits of fluorescence based screens, recent work has expanded the analytical techniques that can be applied to the active sorting of droplets. UV-Vis absorbance,[13, 19] droplet imaging,[20] and Raman spectroscopy[21, 22] have been employed as alternatives to fluorescence detection in droplets. Although these methods have widened the range of analytical techniques available for droplet sorting, they too have significant limitations in their implementation. Raman spectroscopy allows label-free detection of the target analyte but the signal is negatively affected by interference from the oil phase and optical distortion in the droplets. Raman additionally suffers low sensitivity without the use of surface enhancement, which makes the technique more difficult to apply in complex matrices where non-specific molecular adsorption to the necessary metal nanostructures can limit analytical utility.[9, 21, 23]

Absorbance spectroscopy (AADS) offers another unlabeled approach to droplet detection. However, it is both less specific and less sensitive than FADS, necessitating the use of secondary reporters for detection when the target analyte absorbs weakly and when the reaction does not result in a sufficient change in absorbance.[13] Droplet imaging techniques

[a] D. Holland-Moritz, Prof. R.T. Kennedy
Dept. of Chemistry, University of Michigan
930 N University, Ann Abor MI 48109
E-mail: rtkenn@umich.edu
[b] M. Wismer
Scientific Engineering and Design
Merck & Co., Inc.
2000 Galloping Hill Road, Kenilworth, NJ 07033, USA
[c] Dr. P. Devine, Dr. E. Guetschow, Dr. I Mangion, Dr. B. Mann, Dr. J. Moore, Dr. S. Sun
Process Research and Development
Merck & Co., Inc.
126 E. Lincoln Ave, Rahway, NJ 07065, USA
E-mail: Jeffrey_Moore@merck.com
E-mail: shuwen.sun@merck.com
[d] Dr. I. Farasat
Janssen R&D
1400 McKean Rd., PA,19477
[e] Dr. C. Welch
Indiana Consortium Analyt Sci & Engn
Indianapolis, IN 46202 USA.

Supporting information for this article is given via a link at the end of the document.
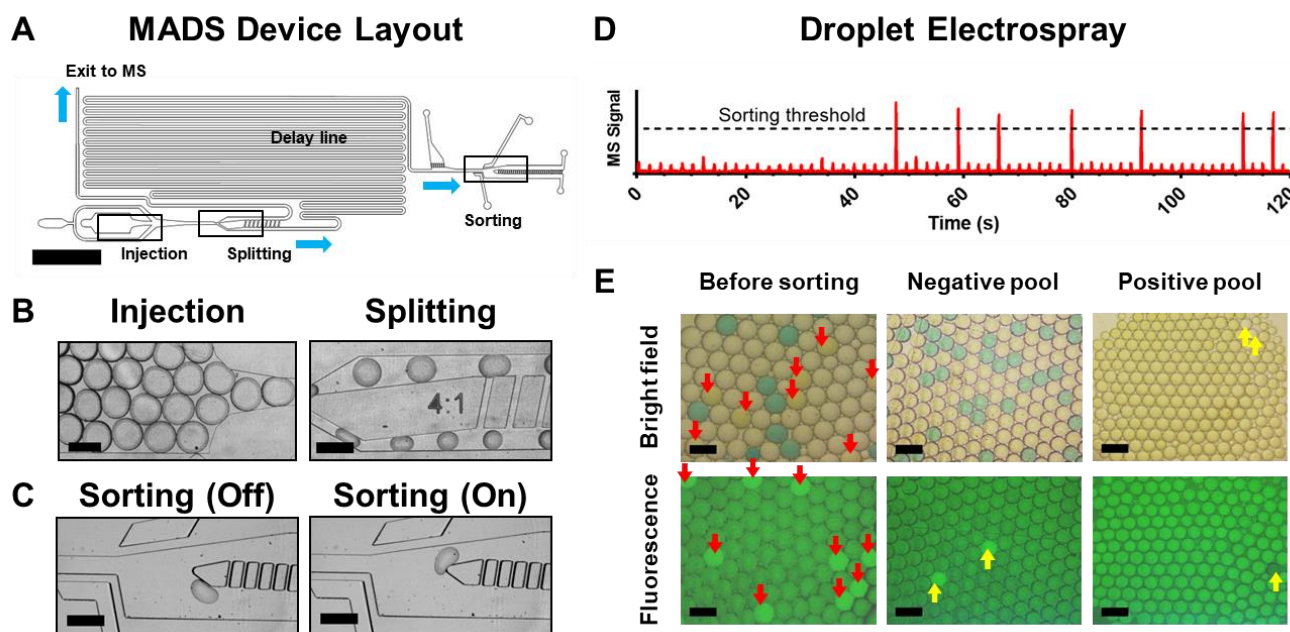
Figure 1. (A) The MADS device schematic is shown with a 5 mm scale bar and arrows indicating flow direction. Droplet samples enter the device in the lower left region labeled "injection" and are split asymmetrically. One portion flows to the mass spectrometer (MS) for analysis. The other portion flows through a delay line to allow time for the MS analysis, and then a dielectrophoretic (DEP) sorter for collection of active droplets. Detailed operation is given in text. (B) Micrographs of the regions for droplet injection and splitting highlighted in A. (C) Micrographs of the DEP sorting junction highlighted in A. (D) At the MS, ~15 nL daughter droplets are analyzed. The resultant trace shows a peak for each droplet that is used to inform the sorting decision of the smaller daughter droplet left behind on the chip. Multiple analytes may be monitored in each droplet, allowing for complex chemical information to be derived from each sprayed sample. (E) In development experiments, sorting is confirmed with image analysis. In this instance, "positive" droplets containing a high concentration of analyte (red arrows) are separated from low analyte concentration "negative" droplets and blue marker droplets based on MS analysis. Fluorescent markers in positive droplets, which appear yellow in bright field images, confirm the accuracy of the sorting. To aid visualization, false positives and false negatives are highlighted with yellow arrows. All scale bars, unless otherwise noted, are 500 μm.

are limited to visible characteristics such as size, color, or particle content, none of which are direct methods for observing the chemical content of a droplet sample.

Analysis and sorting of droplets using mass spectrometry (MS) would be a valuable addition to the methods for droplet sorting. MS offers nearly universal label-free detection with high sensitivity and selectivity, as well as the flexibility for multiplexing. Recent work with ESI[2, 24] and matrix-assisted laser desorption/ionization (MALDI) MS[25] has shown that MS can be used for droplet analysis; however, sample destruction by ESI has been an obstacle to coupling it to microfluidic droplet sorting.

Here, we present Mass Activated Droplet Sorting (MADS), a technique that couples droplet ESI-MS to DEP sorting. MADS is capable of sorting thousands of nanoliter droplets at ~0.7 samples/s based on their MS signal with up to 98% accuracy. The method relies on a programmable sorting algorithm that enables MS-based sample identification and dynamic thresholding.[26]

The utility of this system is first demonstrated by sorting a pool of droplets based on 1-(pyridin-3-yl)ethan-1-amine
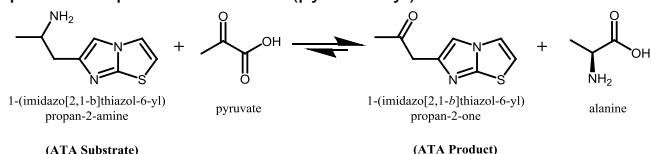
Scheme 1. The reaction for the transformation of the non-native ATA Substrate into its corresponding ATA product ketone is shown, as catalyzed by ATA 117. Early experiments (such as described in Figure 1) used pyridinyl amine as a target analyte. Later experiments used enzymatic reactions according to the reaction above.

(pyridinyl amine, Table S1) concentration. Following this, we screen samples for activity of the transaminase ATA-117 after *in vitro* expression (ivTT) in droplets. We enrich droplets based on their conversion of the non-native substrate 1-(imidazo[2,1-b]thiazol-6-yl) propan-2-amine propan-2-amine (ATA Substrate, Scheme 1). This screen would not be feasible by either FADS or AADS methodology, illustrating the potential of MADS to screen reactions that are not accessible by other methods.

Results and Discussion

The destruction of sample during ESI renders impossible the direct sorting of material that has been analyzed by MS. We have addressed this challenge by asymmetrically splitting the droplets[27] and performing analysis and sorting on the two different portions (Figure 1). In this approach, ~25 nL droplets are pumped from a storage chamber (Figure S1) and onto the chip (Figure 1B), where they are split into two daughter droplets (Video S1). The larger of the two daughter droplets flows into PFA capillary that is mated to a single quadrupole mass spectrometer via a sheath-flow ESI-MS source, where it is directly analyzed without the need for oil removal.[2, 28] The smaller of the two daughter droplets travels into an on-chip delay line to allow time for its sister droplet to reach the mass spectrometer (Figure 1A, Figure S2). The smaller sister droplet may be deflected into the appropriate exit using DEP (Figure 1C) once the larger daughter droplet has been analyzed (Figure 1D) and a sorting decision made. For testing, the accuracy of the system is determined by collecting and imaging the sorted droplets after each experiment (Figure 1E).
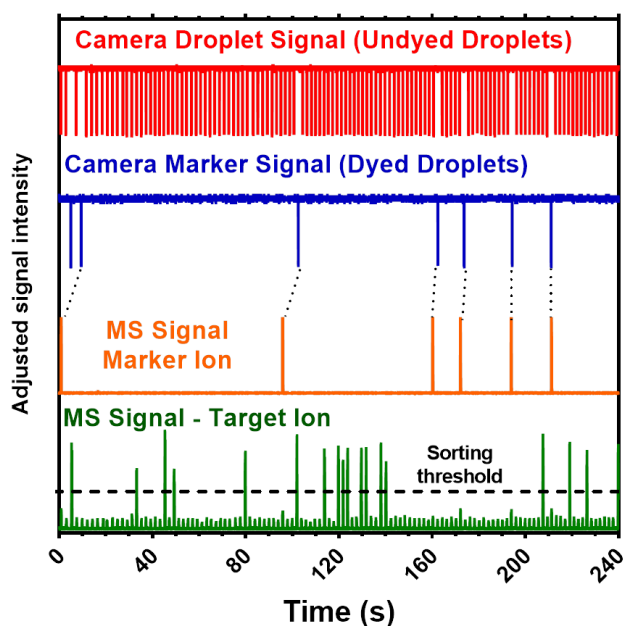
Figure 2 The droplet trace from the mass spectrometer monitoring two distinct ions is plotted with the traces from the digital output of the camera. Sample droplets are uncolored and are recognized by the camera based on pattern recognition (red trace). Marker droplets are colored with food dye and their detection triggers a signal on a second output channel (blue trace). This signal matches with the MS signal from the marker droplet ion (orange trace). A software tool synchronizes the pattern from the two droplet streams, and upon synchronization it uses the signal from the target ion (green trace) to make a sorting decision for each droplet.

Sorting Strategy

In principle, accurate droplet sorting could be achieved either by counting the samples detected by MS and aligning that count to the samples at the DEP junction, or by setting a time delay between the signal on the MS and the DEP pulse that matches the delay between electrospray and sorting. In practice, neither of these strategies is sufficiently stable. The time delay approach is problematic because slight differences in droplet size, spacing and velocity will tend to result in sorting errors. A simple counting approach is problematic because a single miscounted event can result in a frame shift where every subsequent sample is sorted incorrectly.

We used a modified counting approach in which "marker" droplets were randomly mixed with the sample droplets so that the system could proofread its counting (Figure 2). To match the droplet entering the DEP sorting junction with its corresponding mass spectrometer signature, a camera monitors droplets as they enter the sorting region. The camera has image processing capabilities that allow it to trigger a digital signal based on droplet color. The marker droplets contain a unique mass analyte that is monitored by the mass spectrometer and a colored dye that is recognized by the camera. The signal given by marker droplets is used to synchronize the mass spectrometer data with the sorted droplet stream.

The microcontroller software driving the sorting decisions uses a real-time operating system (RTOS) that runs several processes in parallel (Figure S3). The first process acquires

analog input signals from a modified digital to analog converting board installed in the mass spectrometer (Figure S4). A peak detection algorithm identifies peaks on each input signal and records the maximum value for each peak. The magnitudes of these values are then used to classify the peaks and determine which are markers, and which will be targeted for sorting. This data is stored in a queue of virtual droplets. The second process simultaneously monitors the digital output from the camera, classifying the droplets as markers or non-markers based on the output signal. The third process handles communication with the host PC, allowing the user to set sorting parameters and read real-time sorting statistics.

The system synchronizes the mass spectrometer and camera droplet streams by monitoring the intervals between marker droplets in each. It starts operation with all droplets directed to waste. As droplets start flowing past the camera junction, the system counts the number of non-marker droplets between marker droplets. Once the system detects an interval at the camera that matches an interval of virtual droplets stored in the queue, it enters the synchronized state. In this state, the stored droplet information is used to make sorting decisions about the droplets detected at the camera. The system will continue to monitor the intervals between marker droplets, and if the interval between marker droplets ever differs from the interval in the queue by more than three samples (SI, Error Tolerance), the system enters the non-synchronized state. It then attempts to re-synchronize, starting with the next interval. The system is thereby self-correcting and capable of responding to anomalous events such as merged or split droplets that can cause miscounting.

In most experiments we aimed for a marker frequency of about 20%, because the frequent re-alignment (an average of one in five droplets) provides a regular check for the system to ensure it continues to sort accurately. However, the frequency of these markers is flexible and we have observed successful sorting with as low as 7% markers. At higher marker frequencies, a minimum alignment interval length may be set below which the microcontroller will not attempt to align. This reduces the chance of alignment to duplicate intervals, which become more common with increased marker frequency.

Sorting Accuracy

To assess the efficacy of the MADS device and its supporting software, we generated, mixed, and sorted three types of ~25 nL droplets. The bulk (~70-80%) of the droplets contained 50 µM pyridinyl amine (Table S1). Approximately 10% of the droplets contained 500 µM pyridinyl amine (a tenfold increase in target signal) and flavin adenine dinucleotide (FAD). These latter droplets served as high-signal targets for sorting. Although it is not used to make sorting decisions, the FAD is both visibly yellow and fluorescent, allowing sorting accuracy to be evaluated and confirmed by imaging after each experiment. The final 10-20% of the samples contained 500 µM ATA Substrate as a marker ion and blue food dye. These served as markers for sorting alignment.

The mixed population of droplets was pumped onto a sorting device where samples were split and sorted based on the signal from the pyridinyl amine. The threshold for sorting was manually set based on the signal intensity observed for the low

and high concentration of pyridinyl amine. Sorted droplets were collected and imaged to analyze the accuracy of the sorting system. Table 1A summarizes five representative sorting experiments. In all of these experiments, false positive rates in the collected droplets were <12%, and false negative rates were <5%.

We hypothesize that the majority of false negatives are collected during periods in which the microcontroller is in the non-synchronized state, directing all samples to waste, and that the majority of false positives occur when the microcontroller directing the sorting operation becomes misaligned. The microcontroller will synchronize as soon as it recognizes a marker to marker interval on the camera that matches an interval stored in the queue of droplet data from the MS signal. If it aligns to an incorrect interval or miscounts, it will sort incorrectly until it recognizes a subsequent marker signal that does not match the expected interval, enters the non-synchronized state and attempts to realign. We observed that misalignment and non-synchronized periods were often preceded by false sorting events.

Table 1. Sorting results from five representative droplet experiments with and without ivTT.

Experiment	Before Sorting			After Sorting	
	Samples Screened	Hit droplets in initial pool (%)	Marker droplets (%)	Hit droplets in positive pool (%)	Hit droplets in negative pool (%)
A. Target Analyte in Water					
Experiment A	4159	4.7	7.2	88.5	0.9
Experiment B	4444	7.4	11.8	91.7	3.1
Experiment C	3625	9.8	18.8	91.6	4.1
Experiment D	3660	10.8	20.1	96.0	2.9
Experiment E	4001	11.0	20.1	98.7	1.5
B. *In vitro* Expression and Transaminase Assay					
Experiment F	4292	9.9	18.8	93.0	3.1
Experiment G	2340	11.1	10.1	91.0	5.3
Experiment H	2637	9.8	17.2	97.5	3.1
Experiment I	2562	10.5	20.1	94.5	4.8
Experiment J	2067	10.3	20.4	90.5	3.5

In vitro Expression Assay

Our results in the initial investigation of sorting efficiency demonstrated that MADS was capable of sorting mixtures of droplet samples based on their chemical contents with a high degree of accuracy. However, these early tests were conducted with samples containing binary levels of the analyte of interest. We recognized that, in a typical screening scenario, these samples would neither be as simple as analyte-in-water, nor would hits be as discrete (a tenfold difference in concentration).

To test the feasibility of the MADS device for use in a directed evolution workflow, we aimed to sort a model library of droplet samples that contained *in vitro* expressed wildtype (WT) transaminase ATA117, from *Arthrobacter* sp. KNK168 (SI, "Transaminase Plasmid"). This transaminase is the same enzyme starting point that was previously evolved to produce the amine sitagliptin from a ketone.[18] The WT enzyme is fairly promiscuous, and can convert the non-native ATA Substrate amine that we used as a marker ion in our early experiments into ATA Product ketone 1-(imidazo[2,1-b]thiazol-6-yl) propan-2-one when the reaction is run in the thermodynamically favored direction (Scheme 1). The transformation results in a net mass

shift of 1 amu, and none of the substrates or products of the reaction are distinguishable optically in the reaction mix without chromatography.

Initially, we planned to monitor the production of the ketone product in droplets. However, early droplet based ivTT experiments revealed that the ketone product of the transaminase reaction transferred rapidly between droplet samples, making active and inactive samples difficult to distinguish (Figure S5). This type of molecular transfer has been reported previously. [16, 29] The ATA Substrate is more effectively retained within the droplet samples, such that active transaminase in a droplet results in a clear drop in the ATA Substrate signal. Given this data, we elected to monitor reaction progress by observing the reduction of the ATA Substrate.

Droplet MS Dynamic Range

To assess the ability of droplet MS to quantitatively distinguish between varied concentrations of ATA Substrate in complex ivTT matrices, droplets were made from New England Biolab's PURExpress cell free expression mixture. This solution is a complex mixture of proteins, nucleic and amino acids and buffer that contains all the cellular components necessary to transcribe and translate DNA to protein in vitro, and has been used in droplet based directed evolution workflows to express and screen enzyme libraries in droplets.[12]

To test the ability of the MS to track the reaction in ivTT, six solutions were doped with ATA Substrate amine at concentrations from 50 μM to 5 mM and then segmented into 30 nL droplets. These droplet samples were pumped onto the analysis device one concentration at a time (Figure 3A). Signal intensities for each sprayed droplet were extracted for 225 peaks at each concentration and plotted (Figure 3B), showing a linear response to ATA Substrate concentration with a limit of detection of 30 μM.

To demonstrate the capability of the MS to distinguish between these droplets in a mixture, the droplets were mixed and sprayed after an hour of incubation. The raw trace and binned ion intensity for the mixed droplets are shown in Figure 3C and 3D. The histogram of droplet signal intensities shows resolution of each of the six underlying concentrations of ATA Substrate amine in the droplets. These histograms exhibit some drift towards the center when compared to those generated from the sequential spray experiment (Figure S6), possibly due to a small degree of substrate transfer between droplets. Nevertheless, this data may be used to calculate the Z' factor for a potential screen of samples starting at 1 mM and running to 95% conversion (50 μM), giving a Z' of 0.757. This result demonstrates the ability of the MS to identify a wide range of analyte concentrations in droplets containing complex, practical sample, and the potential to sort these populations based on MS signal.
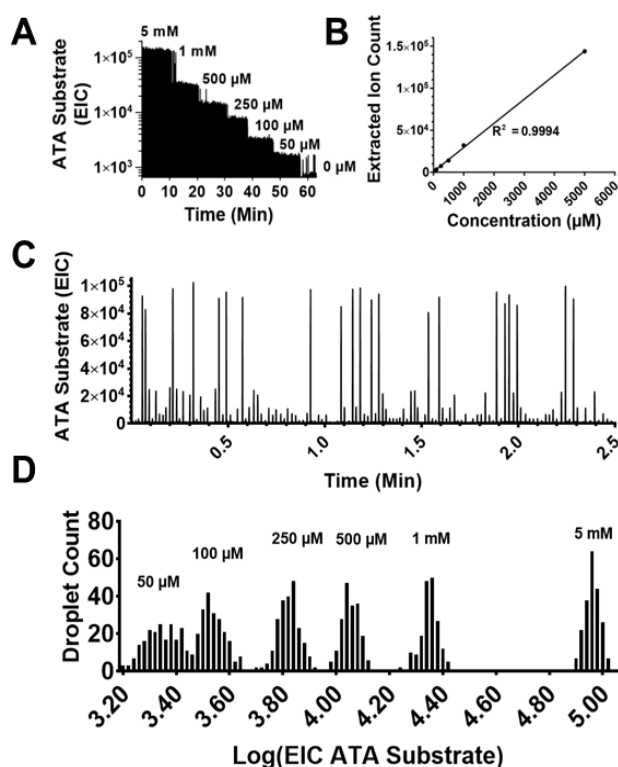
Figure 3 (A) Six concentrations of ATA Substrate amine in droplets of ivTT are sprayed sequentially and (B) the averaged extracted ion count (EIC) from 225 peaks in each population show a linear response with increasing substrate. Error bars show standard error of the mean peak height, which at these scales are all smaller than marker size. After mixing, these same droplets were sprayed (C) and were still distinguished as distinct populations within the whole (D).

Adaptive Thresholding Techniques

Signal drift can affect sorting accuracy if a fixed MS signal threshold is used as the sorting criteria. In our early experiments with DNA bearing ivTT droplets, we observed two forms of MS signal drift. First, enzymatic activity in droplets is not quenched at the initiation of analysis. Figure 4A illustrates the change over 24 h in substrate and product in a bulk reaction of expression and enzymatic turnover. The same occurs in droplets and can be seen as an increasing difference in target signal between inactive and active droplet signals over several hours of a screen (Figure 4B).

Second, we also observed a more gradual drift in the maximum MS intensity of the ATA Substrate in our system, which declined by 15-20% over 6 h. Significantly, the signal for the marker ions remained stable during this same period (Figure S7), suggesting that the signal loss was specific to the ATA Substrate. We theorized that it stemmed from the slow transfer of ATA Substrate from the inactive droplets in the system to those expressing active protein. These two mechanisms for change in signal over time indicate the need to account for this signal drift during long analysis.

To maintain accuracy over time, we developed an "adaptive thresholding" technique to change the threshold for selection as signal drift occurred (Figure S3B). In this modified algorithm, hits are defined in comparison to the running average (16 samples) of a set of positive control signals mixed into the screened population. These positive control samples can be marked with a unique ion that distinguishes them from the sample population, allowing the algorithm to avoid sorting them as hits. We used chlorocholine and neostigmine (Table S1) to
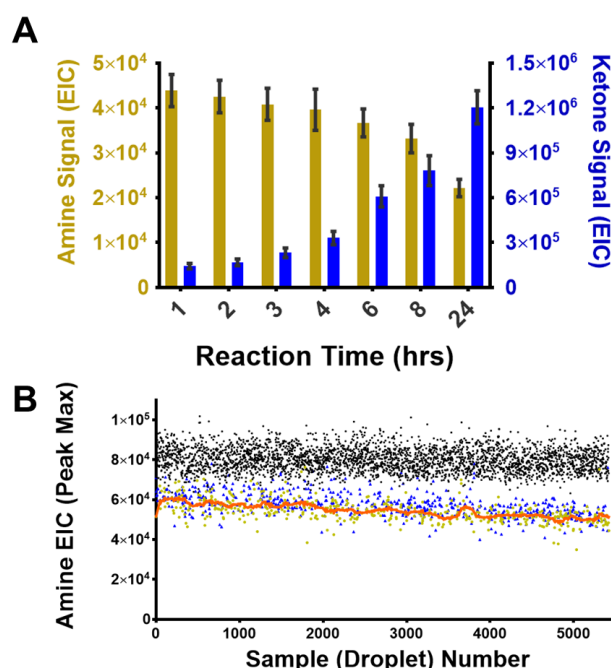
mark the positive control samples and the model library samples respectively; these quaternary amines are robustly contained within droplets and readily ionize under ESI conditions.

In the adaptive mode of operation, the program will only attempt to collect samples marked by the presence of neostigmine. The threshold defaults to the average signal of the samples containing chlorocholine (Figure 4B, orange line), but may be adjusted to be more or less stringent using a multiplier, termed the "sorting ratio". Increasing the sorting ratio raises the threshold for a hit above the average positive signal (Figure S8), and allows a larger portion of the model library to be targeted.

In-droplet Enzyme Assay and Screen

To demonstrate MADS, we created and screened a model library of transaminase enzymes by in vitro expression. For this

Figure 4 (A) Time course data of the transamination reaction (Scheme 1) performed in bulk solution by *in vitro* expressed transaminase shows that as the reaction proceeds after DNA addition, ATA Substrate signal drops as ketone signal rises. (B) In a 3 h trace of ATA Substrate signal in droplets, the same phenomenon may be observed as a gradual increase in the separation between inactive (black circles) and active droplets containing DNA (Blue and yellow circles). In this plot, active samples are divided into two populations: positive control (yellow circles) and model library (blue circles). The positive control signal can be averaged by the adaptive sorting algorithm (orange trace), and this moving average may be used to set sorting criteria for the model library.

experiment, three types of sample droplet were formed through the electrocoalescence of 1 nL droplets to ~25 nL droplets of ivTT reaction mix and ATA Substrate (Figure 5A, Video S2).[31] When the added 1 nL droplet contained WT DNA, neostigmine, and FAD, a visibly yellow, fluorescent droplet expressing transaminase was produced. These model library samples were targeted for sorting, and the added FAD made it possible to confirm the accuracy of the screen using fluorescent imaging. When the 1 nL addition contained WT DNA and chlorocholine, an active positive control droplet was produced. 1 nL water droplets made up the bulk of the small droplets, and the addition of these produced inactive ivTT samples. Marker droplets for synchronization were generated from ivTT doped with carnitine and blue food dye and were mixed into the final pool of droplet samples.

The microcontroller utilized the running average of the ATA Substrate signal in positive control droplets containing chlorocholine to adjust the sorting threshold. The neostigmine channel was used to identify model library members that would be considered for sorting. The carnitine channel was used to identify marker droplets.

Because all model library droplets were expressing the same WT DNA as the positive control droplets, the default threshold produced by the average wildtype signal only targeted approximately 50% of the active droplets. The sorting ratio was therefore set above 1.0 (Figure S8) in experiments that aimed to recapture all of the model library droplets from the mixed pool. Droplets that showed ATA Substrate signal below this threshold were targeted for sorting, and those that did not were rejected and allowed to flow to waste. In a screening scenario, this cutoff will likely be set to more stringent values to select only for high performance hits.

After 3-4 h incubation (Figure S1)[32] to give the enzyme time to react, the droplets were reinjected and sorted, with samples taken and imaged at 1 or 2 h intervals. A representative trace of the mass signal for the droplets is shown in Figure 5B. Model library droplets show a reduction in ATA Substrate, a high neostigmine signal, and are fluorescent. Positive control droplets show a similar reduction in ATA Substrate but display high chlorocholine signal, and are therefore not targeted for sorting. Marker droplets and droplets that did not receive an addition containing DNA remain unchanged in their ATA Substrate amine concentration.

In all experiments with a sorting ratio above 1.3, the collected droplet pools showed enrichment above 90%, from a starting occupancy of approximately 10%. Table 1B shows the results from 5 experiments with a sorting ratio of 1.45, where 98% of the droplets dosed with DNA, FAD and Neostigmine were targeted for sorting. Collected droplets were imaged and counted using the fluorescence of the FAD to confirm accurate sorting (Figure 5C). Accuracy was found to be on par with our previous experiments using aqueous solutions of known analyte concentration.

The results of this experiment show the capability of the system to perform multiplex analysis in a complex reaction
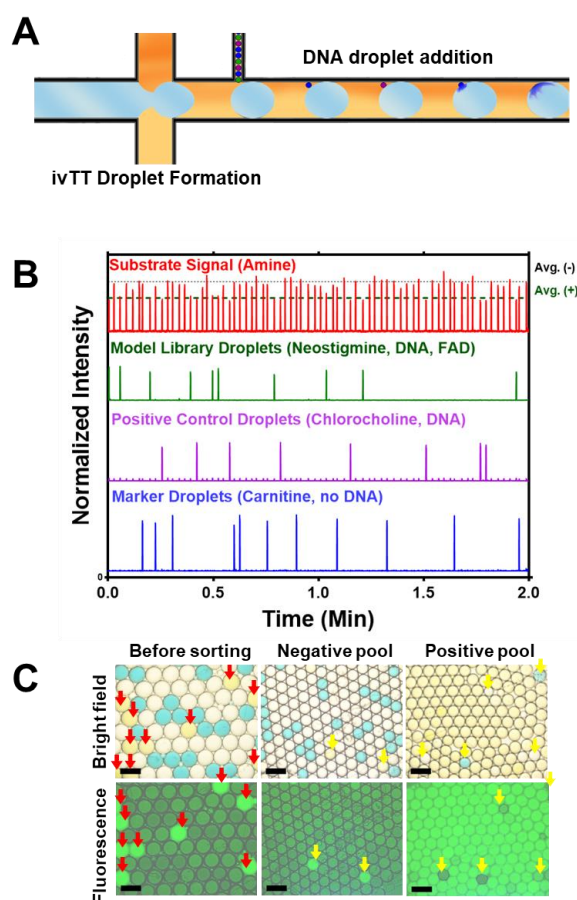
mixture and use information from an ongoing chemical reaction to accurately sort a target population.

Figure 5 (A) A mixture of 1 nL droplets that occasionally contain plasmid DNA with MS traceable analytes are added to 25 nL droplets to create a mixed pool of large droplets where some express active protein(Video S2). (B) The droplets are sprayed, and the small molecule tracers neostigmine and chlorocholine allow the MS to identify those that have received and expressed this DNA. A modified sorting algorithm reads the resultant trace and uses the average amine signal from the droplets containing chlorocholine (purple trace) to set the sorting threshold for those containing neostigmine (green trace). Average positive, shown as Avg.(+), and average negative signals, shown as Avg.(-), are marked to highlight how all droplets containing these two marker signals exhibit the expected drop in Amine signal. (C) Sorting is confirmed with fluorescent imaging of the droplets after they have been collected. Here, model library droplets in the starting pool are highlighted with red arrows, and false positives and negatives in the sorted pools are marked with yellow arrows. Scale bars are 500 µm.

Throughput and Extended Operation

Throughput of MADS was 0.7 samples/s while monitoring 4 ion traces in single ion monitoring mode. This throughput was limited by the time required to collect sufficient data points across a single droplet for accurate analysis. At the maximum scan rate of the MS and using 4 signal channels, ~30 data points/s are collected on a single channel. At the rate of operation used for the experiments described here, the dwell time of a droplet at the spray tip is approximately 0.3 s, allowing

just 10 data points to be collected. Faster scanning mass spectrometers may allow higher throughput.

The MADS system is capable of operating for long periods. We have been able to collect data and sort samples for 6 h, with as many as 10^4 samples analyzed and sorted (Figure S7). We found no inherent reason that longer periods of operation would not be possible.

Conclusion

Although FADS has been the most utilized approach for sorting droplet samples since its introduction[8] and has enabled sorting at throughputs unachievable in conventional systems, indirect assays often lead to off-target selection. [14] A screen that directly interrogates the analyte of interest is far preferable. With careful assay development, both FADS and AADS have been used to screen industrially relevant enzymes, [15] but the vast majority of potential targets will not be amenable to such reporter assays.

Here, we have demonstrated an adaptive, self-correcting MADS system with the ability to screen complex biological reactions. This work links a versatile, label-free analytical tool to microfluidics workflows and significantly broadens the applicability of these miniaturized systems.

The inherent label free nature of MS makes MADS a valuable tool for probing chemistries that cannot be easily adapted to FADS, broadening detection to include most molecules that are readily ionizable with ESI. The resolution of MS also allows numerous analytes to be simultaneously monitored, creating the potential for selective, multifaceted probes of activity. For screening chemical reactions, the ability to detect changes in mass is more broadly applicable than changes in spectra. Although MADS sorting rates are 1000-fold slower than those demonstrated with FADS, they are still 100-fold faster than industry standard HPLC-MS methods. The higher detection limits of MADS as demonstrated are on par with absorbance screens. This should be sufficient for most applications, but could be improved by adapting the method to a triple quadrupole mass spectrometer if desired.

Conflict of Interest

R.T.K. has an interest in a company that seeks to commercialize droplet ESI-MS.

[1]   J. Agresti, E. Antipov, A. Abate, K. Ahn, A. Rowat, J. Baret, M. Marquez, A. Klibanov, A. Griffiths, D. Weitz, *Proceedings of the National Academy of Sciences of the United States of America* **2010**, *107*, 6550-6550.

[2]   X. Diefenbach, I. Farasat, E. Guetschow, C. Welch, R. Kennedy, S. Sun, J. Moore, *Acs Omega* **2018**, *3*, 1498-1508.

[3]   X. Zhu, X. Shi, S. Wang, J. Chu, W. Zhu, B. Ye, P. Zuo, Y. Wang, *Rsc Advances* **2019**, *9*, 4507-4513; A. Klein, L. Mazutis, I. Akartuna, N. Tallapragada, A. Veres, V. Li, L. Peshkin, D. Weitz, M. Kirschner, *Cell* **2015**, *161*, 1187-1201; E. Macosko, A. Basu, R. Satija, J. Nemesh, K. Shekhar, M. Goldman, I. Tirosh, A. Bialas, N. Kamitaki, E. Martersteck, J. Trombetta, D. Weitz, J. Sanes, A. Shalek, A. Regev, S. McCarroll, *Cell* **2015**, *161*, 1202-1214.

[4]   W. Cochrane, M. Malone, V. Dane, V. Cavett, A. Satz, B. Paegel, *Acs Combinatorial Science* **2019**, *21*, 425-435; A. MacConnell, A. Price, B. Paegel, *Acs Combinatorial Science* **2017**, *19*, 181-192.

[5]   Y. Tao, A. Rotem, H. Zhang, C. Chang, A. Basu, A. Kolawole, S. Koehler, Y. Ren, J. Lin, J. Pipas, A. Feldman, C. Wobus, D. Weitz, *Lab on a Chip* **2015**, *15*, 3934-3940; B. DeKosky, T. Kojima, A. Rodin, W. Charab, G. Ippolito, A. Ellington, G. Georgiou, *Nature Medicine* **2015**, *21*, 86-91.

[6]   K. Ahn, C. Kerbage, T. Hunt, R. Westervelt, D. Link, D. Weitz, *Applied Physics Letters* **2006**, *88*.

[7]   J. Baret, O. Miller, V. Taly, M. Ryckelynck, A. El-Harrak, L. Frenz, C. Rick, M. Samuels, J. Hutchison, J. Agresti, D. Link, D. Weitz, A. Griffiths, *Lab on a Chip* **2009**, *9*, 1850-1858; T. Beneyton, I. Wijaya, P. Postros, M. Najah, P. Leblond, A. Couvent, E. Mayot, A. Griffiths, A. Drevelle, *Scientific Reports* **2016**, *6*; M. Najah, R. Calbrix, I. Mahendra-Wijaya, T. Beneyton, A. Griffiths, A. Drevelle, *Chemistry & Biology* **2014**, *21*, 1722-1732.

[8]   S. Sjostrom, Y. Bai, M. Huang, Z. Liu, J. Nielsen, H. Joensson, H. Svahn, *Lab on a Chip* **2014**, *14*, 806-813.

[9]   Y. Zhu, Q. Fang, *Analytica Chimica Acta* **2013**, *787*, 24-35.

[10]   T. Tran, F. Lan, C. Thompson, A. Abate, *Journal of Physics D-Applied Physics* **2013**, *46*.

[11]   O. Caen, S. Schutz, M. Jammalamadaka, J. Vrignon, P. Nizard, T. Schneider, J. Baret, V. Taly, *Microsystems & Nanoengineering* **2018**, *4*; R. Obexer, M. Pott, C. Zeymer, A. Griffiths, D. Hilvert, *Protein Engineering Design & Selection* **2016**, *29*, 355-365; B. Kintses, C. Hein, M. Mohamed, M. Fischlechner, F. Courtois, C. Leine, F. Hollfelder, *Chemistry & Biology* **2012**, *19*, 1001-1009; P. Colin, B. Kintses, F. Gielen, C. Miton, G. Fischer, M. Mohamed, M. Hyvonen, D. Morgavi, D. Janssen, F. Hollfelder, *Nature Communications* **2015**, *6*.

[12]   A. Fallah-Araghi, J. Baret, M. Ryckelynck, A. Griffiths, *Lab on a Chip* **2012**, *12*, 882-891.

[13] F. Gielen, R. Hours, S. Emond, M. Fischlechner, U. Schell, F. Hollfelder, *Proceedings of the National Academy of Sciences of the United States of America* **2016**, *113*, E7383-E7389.

[14] E. Farinas, T. Bulter, F. Arnold, *Current Opinion in Biotechnology* **2001**, *12*, 545-551.

[15] A. Debon, M. Pott, R. Obexer, A. Green, L. Friedrich, A. Griffiths, D. Hilvert, *Nature Catalysis* **2019**, *2*, 740-747.

[16] Y. Chen, A. Gani, S. Tang, *Lab on a Chip* **2012**, *12*, 5093-5103; F. Courtois, L. Olguin, G. Whyte, A. Theberge, W. Huck, F. Hollfelder, C. Abell, *Analytical Chemistry* **2009**, *81*, 3008-3016.

[17] Y. Skhiri, P. Gruner, B. Semin, Q. Brosseau, D. Pekin, L. Mazutis, V. Goust, F. Kleinschmidt, A. El Harrak, J. Hutchison, E. Mayot, J. Bartolo, A. Griffiths, V. Taly, J. Baret, *Soft Matter* **2012**, *8*, 10618-10627.

[18] C. Savile, J. Janey, E. Mundorff, J. Moore, S. Tam, W. Jarvis, J. Colbeck, A. Krebber, F. Fleitz, J. Brands, P. Devine, G. Huisman, G. Hughes, *Science* **2010**, *329*, 305-309.

[19] R. Maceiczyk, D. Hess, F. Chiu, S. Stavrakis, A. deMello, *Lab on a Chip* **2017**, *17*, 3654-3663.

[20] M. Girault, H. Kim, H. Arakawa, K. Matsuura, M. Odaka, A. Hattori, H. Terazono, K. Yasuda, *Scientific Reports* **2017**, *7*; E. Zang, S. Brandes, M. Tovar, K. Martin, F. Mech, P. Horbert, T. Henkel, M. Figge, M. Roth, *Lab on a Chip* **2013**, *13*, 3707-3713.

[21] C. Syme, C. Martino, R. Yusvana, N. Sirimuthu, J. Cooper, *Analytical Chemistry* **2012**, *84*, 1491-1495.

[22] X. Wang, L. Ren, Y. Su, Y. Ji, Y. Liu, C. Li, X. Li, Y. Zhang, W. Wang, Q. Hu, D. Han, J. Xu, B. Ma, *Analytical Chemistry* **2017**, *89*, 12569-12577.

[23] I. Jahn, O. Zukovskaja, X. Zheng, K. Weber, T. Bocklitz, D. Cialla-May, J. Popp, *Analyst* **2017**, *142*, 1022-1047.

[24] S. Sun, R. Kennedy, *Analytical Chemistry* **2014**, *86*, 9309-9314; C. Smith, X. Li, T. Mize, T. Sharpe, E. Graziani, C. Abell, W. Huck, *Analytical Chemistry* **2013**, *85*, 3812-3816; K. Wink, L. Mahler, J. Beulig, S. Piendl, M. Roth, D. Belder, *Analytical and Bioanalytical Chemistry* **2018**, *410*, 7679-7687; D. J. Steyer, R. T. Kennedy, *Analytical Chemistry* **2019**, *91*, 6645-6651; S. Sun, T. Slaney, R. Kennedy, *Analytical Chemistry* **2012**, *84*, 5794-5800.

[25] S. Kuster, S. Fagerer, P. Verboket, K. Eyer, K. Jefimovs, R. Zenobi, P. Dittrich, *Analytical Chemistry* **2013**, *85*, 1285-1289; S. Kuster, M. Pabst, K. Jefimovs, R. Zenobi, P. Dittrich, *Analytical Chemistry* **2014**, *86*, 4848-4855; T. Hatakeyama, D. Chen, R. Ismagilov, *Journal of the American Chemical Society* **2006**, *128*, 2518-2519.

[26] H. Lee, M. Crane, Y. Zhang, H. Lu, *Integrative Biology* **2013**, *5*, 372-380.

[27] J. Nie, R. Kennedy, *Analytical Chemistry* **2010**, *82*, 7852-7856.

[28] J. Pei, Q. Li, M. Lee, G. Valaskovic, R. Kennedy, *Analytical Chemistry* **2009**, *81*, 6558-6561.

[29] M. Pan, L. Rosenfeld, M. Kim, M. Xu, E. Lin, R. Derda, S. Tang, *Acs Applied Materials & Interfaces* **2014**, *6*, 21446-21453; M. Pan, F. Lyu, S. Tang, *Analytical Chemistry* **2015**, *87*, 7938-7943; G. Etienne, A. Vian, M. Biocanin, B. Deplancke, E. Amstad, *Lab on a Chip* **2018**, *18*, 3903-3912.

[30] J. Zhang, T. Chung, K. Oldenburg, *Journal of Biomolecular Screening* **1999**, *4*, 67-73.

[31] K. Ahn, J. Agresti, H. Chong, M. Marquez, D. Weitz, *Applied Physics Letters* **2006**, *88*.

[32] L. Mahler, M. Tovar, T. Weber, S. Brandes, M. Rudolph, J. Ehgartner, T. Mayr, M. Figge, M. Roth, E. Zang, *Rsc Advances* **2015**, *5*, 101871-101878.

[33] F. Ma, M. Chung, Y. Yao, R. Nidetz, L. Lee, A. Liu, Y. Feng, K. Kurabayashi, G. Yang, *Nature Communications* **2018**, *9*.

RESEARCH ARTICLE

We describe a microfluidic system for sorting nanoliter droplets based on mass spectrometry. Fully automated, label free sorting at 0.7 samples/s is achieved with 98% accuracy. In vitro transcription and translation (ivTT) of a transaminase enzyme in ~25 nL samples is demonstrated and samples are sorted on enzyme activity.

Droplet Sampling

Droplet Mass Spectrometry

Mass Activated Droplet Sorting
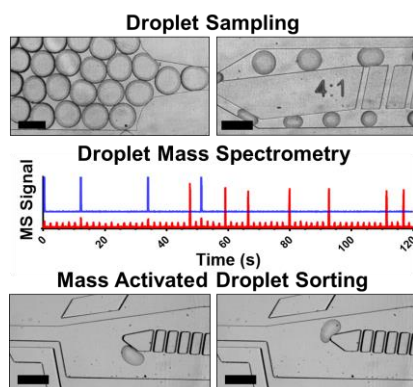
Daniel A. Holland-Moritz, Michael Wismer, Benjamin F. Mann, Iman Farasat, Paul Devine, Erik D. Guetschow, Ian Mangion, Christopher J. Welch, Jeffrey C. Moore, Shuwen Sun, and Robert T. Kennedy

Page No. – Page No.

Mass Activated Droplet Sorting (MADS) Enables High Throughput Screening of Enzymatic Reactions at Nanoliter Scale

Keywords: Biocatalysis • Droplet Microfluidics • High throughput Screening • Mass Spectrometry • Microreactors